

## Annulations

International Edition: DOI: 10.1002/anie.201604741  
German Edition: DOI: 10.1002/ange.201604741

## Pyrenes, Peropyrenes, and Teropyrenes: Synthesis, Structures, and Photophysical Properties

Wenlong Yang, Jorge H. S. K. Monteiro, Ana de Bettencourt-Dias, Vincent J. Catalano, and Wesley A. Chalifoux\*

**Abstract:** The design of a relatively simple and efficient method to extend the  $\pi$ -conjugation of readily available aromatics in one-dimension is of significant value. In this paper, pyrenes, peropyrenes, and teropyrenes were synthesized through a double or quadruple benzannulation reaction of alkynes promoted by Brønsted acid. This novel method does not involve cyclodehydrogenation (oxidative aryl–aryl coupling) to arrive at the newly incorporated large arene moieties. All of the target compounds were synthesized in moderate to good yields and were fully characterized with the structures unambiguously confirmed by X-ray crystallography. As expected, photophysical characterization clearly shows increasing red-shifts as a function of extended conjugation within the fused ring systems.

Well-defined, nanosized polycyclic aromatic hydrocarbons (PAHs) have attracted significant interest because of their wide use in electronic and optoelectronic devices, including organic light-emitting diodes (OLEDs), organic field-effect transistors (OFETs), and in solar cell applications.<sup>[1]</sup> In particular, the bottom-up synthesis of PAHs which can be recognized as nanographenes or graphene nanoribbon (GNR)-type segments has sparked considerable interest in many fields because of their interesting optical and electronic properties.<sup>[2]</sup> The most common approach used to prepare these PAHs is an oxidative aryl–aryl bond-forming reaction (the Scholl reaction) as the key C–C bond-forming step.<sup>[3]</sup> However, this reaction does not work well for making functionalized PAHs because of undesired rearrangements which occur under these harsh reaction conditions.<sup>[4]</sup> The development of a synthetic protocol to arrive at functionalized and soluble pyrenacenes (homologues of pyrene) such as pyrene, peropyrene, and teropyrene derivatives, which can be viewed as fundamental 5-armchair edge GNR (5-AGNR) oligomers (Figure 1), would therefore be of significant value. Pyrene itself has been widely investigated because of its commercial availability and easy modifiability. Therefore, plenty of  $\pi$ -extended derivatives can be synthesized using pyrene as a building block.<sup>[5]</sup> Peropyrene has attracted recent attention because of its fascinating photophysical properties.

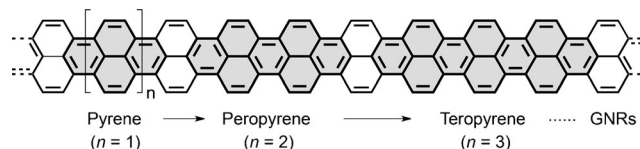


**Figure 1.** Homologues of pyrene (“pyrenacenes”) superimposed on a 5-AGNR.

For example, Bardeen and co-workers assessed its potential use as a singlet fission material, thus pointing out that including substituents on peropyrene should improve peropyrene’s singlet fission properties.<sup>[6]</sup> However, a good method to introduce substituents onto peropyrene to improve its physical properties is still lacking. As the next longer analogue, teropyrene is expected to exhibit a bathochromic shift in both absorption and emission bands with respect to both pyrene and peropyrene, as well as a lower band gap owing to its extended  $\pi$  system. In 1975, Misumi and co-workers reported the first teropyrene synthesis from multi-layered metacyclophanes by a transannular reaction/dehydrogenation sequence, and it was characterized only by its absorption spectrum because of poor solubility.<sup>[7]</sup> Bodwell and co-workers reported the synthesis of a series of bent teropyrenes (teropyrenophanes) and fully characterized them spectroscopically with the structures unambiguously confirmed by X-ray crystallography.<sup>[8]</sup> Cyclodehydrogenation/oxidation was the key step for the synthesis of all of these compounds. The difficult preparation, poor solubility, and difficulty associated with the functionalization of peropyrene and teropyrene have seriously hindered the scientific community’s ability to probe the properties of these materials and to explore their use in electronic and optoelectronic applications. Therefore, the development of new methods which are suitable for the synthesis of functionalized as well as soluble pyrenacenes such as pyrene and more importantly peropyrene and teropyrene derivatives is highly desirable.

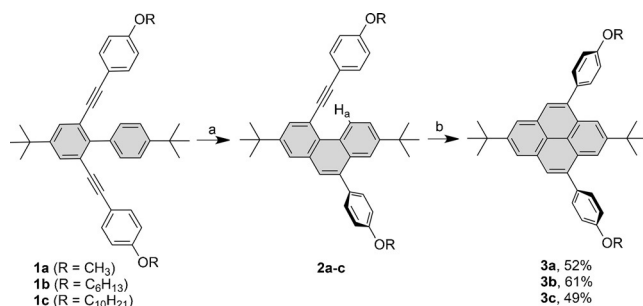
Alkyne benzannulation reactions have been shown to proceed using a variety of  $\pi$ -Lewis acids such as gold(III),<sup>[9]</sup> platinum(II),<sup>[10]</sup> ruthenium(II),<sup>[10b,c]</sup> indium(III),<sup>[10b,11]</sup> and antimony(V).<sup>[12]</sup> Brønsted acids and some other electrophiles, such as ICl, I<sub>2</sub>, and NBS have also been used for alkyne benzannulation reactions.<sup>[13]</sup> 4,10-Disubstituted pyrenes were successfully synthesized through a gold(I)- or platinum(II)-catalyzed twofold benzannulation reaction of 2,6-dialkynylbiphenyls.<sup>[14]</sup> However, neither peropyrenes nor teropyrenes have been prepared through alkyne benzannulation reactions. Herein, we report an efficient approach to generate soluble pyrene, peropyrene, and teropyrene derivatives by a double

[\*] Dr. W. Yang, Dr. J. H. S. K. Monteiro, Prof. A. de Bettencourt-Dias, Prof. V. J. Catalano, Prof. W. A. Chalifoux  
Department of Chemistry, University of Nevada, Reno  
1664 N. Virginia St., Reno, NV 89557 (USA)  
E-mail: wchalifoux@unr.edu

Supporting information and the ORCID identification number(s) for the author(s) of this article can be found under <http://dx.doi.org/10.1002/anie.201604741>.

or quadruple benzannulation reaction of alkynes promoted by a Brønsted acid. With a relatively simple and efficient protocol to access peropyrenes and teropyrenes we can now begin to study these materials in more depth as well as assess their suitability in a host of applications.

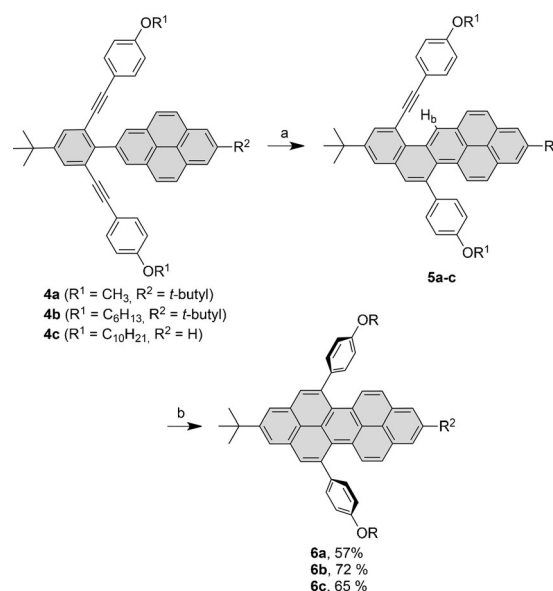
We first considered a quick and easy preparation of the corresponding precursors for pyrene, peropyrene, and teropyrene. We developed a new method to prepare the 2,6-dialkynylbiphenyls **1** (see the Supporting Information), and this method also made it convenient to explore the synthesis of larger  $\pi$ -system compounds. We first treated **1a** with TFA in anhydrous  $\text{CH}_2\text{Cl}_2$  at room temperature (Scheme 1). After



**Scheme 1.** Synthesis of the pyrene derivatives **3**. Reagents and conditions: a) TFA,  $\text{CH}_2\text{Cl}_2$ , RT; b) TfOH,  $\text{CH}_2\text{Cl}_2$ ,  $0^\circ\text{C}$ . TFA = trifluoroacetic acid, Tf = trifluoromethanesulfonyl.

2 hours, only the monocyclized product, phenanthrene derivative **2a**, was formed and was fully characterized by NMR and IR spectroscopy, as well as HRMS. The  $^1\text{H}$  NMR spectrum of **2a** showed a doublet at  $\delta = 10.3$  ppm, which is assigned to the proton in the “bay” position of the newly formed phenanthrene ( $\text{H}_a$ ; Scheme 1). This extreme deshielding is attributed to the planarized phenanthryl geometry formed in **2a** after the first cyclization, which places  $\text{H}_a$  directly in the deshielding zone of the remaining alkyne.<sup>[15]</sup> Only a trace amount of the pyrene derivative **3a** was formed with the addition of excess TFA (100 equivalents) after 24 hours at room temperature. When **1a** was refluxed in dichloroethane in the presence of excess TFA (100 equivalents) for 2 days, **3a** was formed in higher yield but **2a** was still detected in an appreciable amount. We found that by adding a stronger acid, such as TfOH, rapid cyclization of the remaining alkyne occurred.<sup>[13d]</sup> When cyclizing **1a** with only TfOH we observed side products and lower yields. Our optimal reaction conditions consisted of using TFA first to cleanly provide **2a** and subsequent addition of TfOH at  $0^\circ\text{C}$  to cyclize the remaining alkyne. This method provided pyrene derivatives **3a-c** in moderate yields.

With optimized reaction conditions in hand we looked at applying our double alkyne cyclization method to target larger PAH fragments such as peropyrene. Compounds **4a-c** (Scheme 2) were synthesized in an analogous manner as **1a-c** (see the Supporting Information). Upon treatment of **4a-c** with TFA in anhydrous  $\text{CH}_2\text{Cl}_2$  at room temperature, the monocyclized products **5a-c** were formed cleanly. The proton  $\text{H}_b$  in the bay position was diagnostic by  $^1\text{H}$  NMR spectroscopy as it was deshielded to  $\delta \approx 11.1$  ppm. Upon addition of



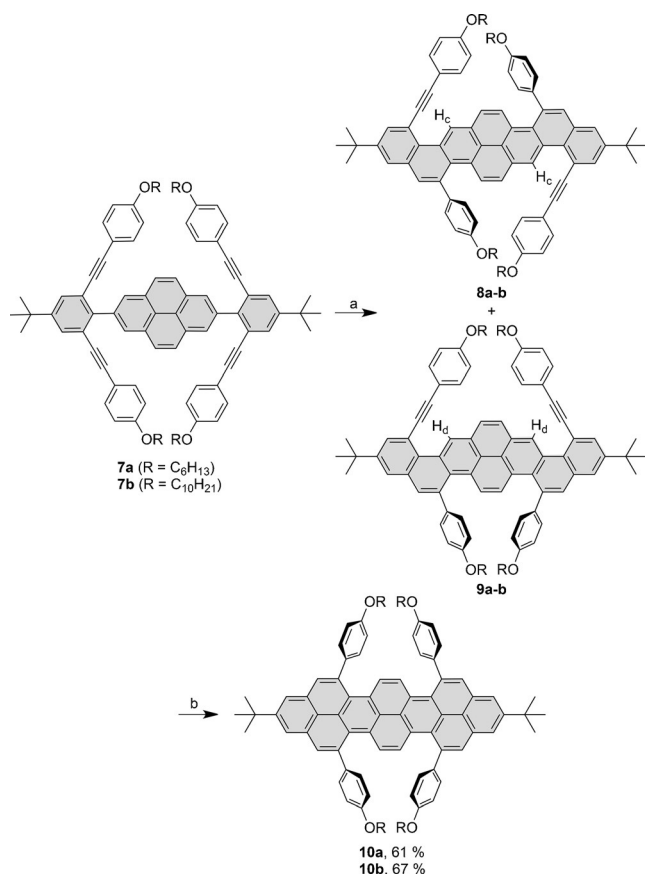
**Scheme 2.** Synthesis of peropyrene derivatives **6a-c**. Reagents and conditions: a) TFA,  $\text{CH}_2\text{Cl}_2$ , RT; b) TfOH,  $\text{CH}_2\text{Cl}_2$ ,  $0^\circ\text{C}$ .

TfOH at  $0^\circ\text{C}$ , the peropyrene derivatives **6a-c** were obtained in moderate to good yield.

With proof-of-concept that we could promote a double alkyne benzannulation to provide pyrene and peropyrene derivatives, we wondered whether a fourfold cyclization would be feasible. Upon treating the compounds **7a** and **7b** with excess TFA at room temperature, we observe the same phenomenon where only one of the two alkynes on each phenyl substituent successfully cyclizes (Scheme 3). This cyclization leads to a mixture of doubly cyclized intermediates **8** and **9** in a 1:2 ratio of isomers (identified by  $^1\text{H}$  NMR spectroscopy and not separated; see the Supporting Information for details). The mixture of **8** and **9** was further reacted with TfOH to afford the corresponding target compounds **10a** and **10b** in 61 and 67% yield, respectively. It should be noted that this yield constitutes roughly an 88–90% yield per alkyne cyclization. What is more remarkable is that these large PAHs show good solubility in many common organic solvents.

Single crystals of **3a**, **6b**, and **10a** suitable for X-ray crystallographic analysis were obtained. The structure of **3a** is relatively flat with the aryl substituents twisted out of conjugation, as expected (Figure 2a). The peropyrene **6b**, on the other hand, shows slight twisting of the PAH core resulting from steric repulsion of the aryl groups and the hydrogen substituents at the bay positions (Figure 2b). This twist results in the peropyrene being axially chiral with an end-to-end twist angle of  $18^\circ$ . The teropyrene **10a** also shows slight twisting of the PAH core resulting from repulsion in the bay region (Figure 2c). In this case the ends are coplanar and the center of the PAH is twisted  $15^\circ$  out of planarity with respect to the ends. In all three structures, the twisting of the aryl substituents out of planarity can explain the absence of  $\pi$ -stacking interactions between neighboring PAHs.

The absorption spectra of **3a**, **6b**, and **10a** are shown in Figure S1 (see the Supporting Information). They absorb in the UV and visible region, and the absorption bands show a characteristic vibrational progression. The increase in



**Scheme 3.** Synthesis of teropyrene derivatives **10a** and **10b**. Reagents and conditions: a) TFA, CH<sub>2</sub>Cl<sub>2</sub>, RT; b) TFOH, CH<sub>2</sub>Cl<sub>2</sub>, 0 °C.

conjugation from **3a**, to **6b** to **10a** is mirrored in the bathochromic shift of the absorption bands and the observed increase in molar absorptivity [ $\epsilon$ ; see Figures S4(a) and S4(b)]. The determined  $\epsilon$  values for **3a** ( $2.2 \times 10^4 \text{ M}^{-1} \text{ cm}^{-1}$  at 352 nm), **6b** ( $5.6 \times 10^4 \text{ M}^{-1} \text{ cm}^{-1}$  at 467 nm), and **10a** ( $2.8 \times 10^5 \text{ M}^{-1} \text{ cm}^{-1}$  at 572 nm) are on the same order of magnitude as for similar reported compounds.<sup>[16]</sup> The excitation and emission spectra are shown in Figure 3. The emission maxima are deep blue at  $\lambda = 392 \text{ nm}$  for **3a**, green at  $\lambda = 486 \text{ nm}$  for **6b**, and red at  $\lambda = 590 \text{ nm}$  for **10a**, and the emission bands for the latter show vibrational fine structure, analogous to the absorption and excitation spectra. The increased conjugation is reflected in the observed bathochromic shift of emission [Figure 3; see Figure S4(c)] as well as the decrease in the Stokes shift (Table 1). The observed emission spectra are mirror images of the excitation and absorption spectra, and indicates that the same states are involved in absorption and emission.

The emission lifetimes and efficiencies for all three compounds, summarized in Table 1, were measured in toluene. The emission lifetimes are  $17.4 \pm 0.1 \text{ ns}$  (**3a**),  $2.5 \pm 0.1 \text{ ns}$  (**6b**), and  $2.5 \pm 0.2 \text{ ns}$  (**10a**), which correspond to emissive rates of 0.0044, 0.2468, and  $0.2444 \text{ ns}^{-1}$ , respectively. All decay curves were fit to a mono exponential (see Figures S6, S8, and S10), thus indicating that emission occurs from one excited state. The emission efficiencies are  $7.7 \pm 0.9\%$  (**3a**),  $61.7 \pm 6.4\%$  (**6b**), and  $61.1 \pm 4.2\%$  (**10a**).

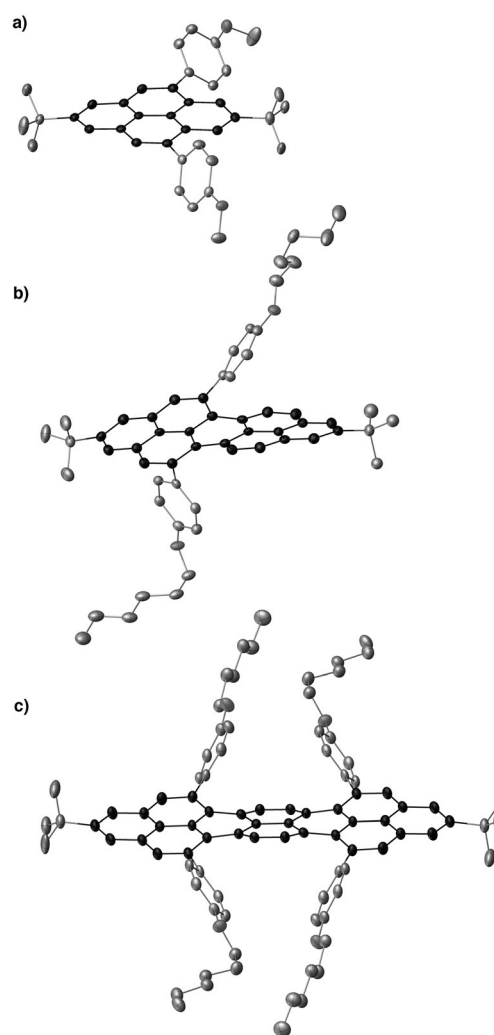


**Figure 2.** Thermal ellipsoid plots (ellipsoids at 50% probability, hydrogen atoms omitted for clarity) of a) the pyrene **3a**, b) the peropyrene **6b** showing an 18° chiral twist of the PAH core, and c) the teropyrene **10a** showing the center of the PAH twisting about 15° out of planarity with respect to the ends.

**Table 1:** Stokes shift, emission lifetimes ( $\tau$ ), radiative rates ( $k_{\text{rad}}$ ), and emission efficiencies ( $\Phi$ ) obtained for the compounds in toluene.

Compound	Stokes shift [cm <sup>-1</sup> ]	$\tau$ [ns]	$k_{\text{rad}}$ [ns <sup>-1</sup> ]	$\Phi$ [%]
Pyrene <b>3a</b>	2540	$17.4 \pm 0.1$	0.0044	$7.7 \pm 0.9$
Pyrene <b>3b</b>	2540	$16.0 \pm 0.1$	0.0053	$8.4 \pm 0.7$
Peropyrene <b>6b</b>	790	$2.5 \pm 0.1$	0.2468	$61.7 \pm 6.4$
Peropyrene <b>6c</b>	800	$2.6 \pm 0.1$	0.2081	$54.1 \pm 2.6$
Teropyrene <b>10a</b>	590	$2.5 \pm 0.2$	0.2444	$61.1 \pm 4.2$
Teropyrene <b>10b</b>	560	$2.6 \pm 0.1$	0.2335	$60.7 \pm 5.0$

The lowest efficiency found for **3a** is a combination of the inefficient absorption and losses resulting from the rotation of the phenyl rings on the side chain. In the case of **6b** and **10a**, the increase in the absorption coefficient (see Figure S1) and the decrease in the lifetime contribute to an increase in the emission efficiencies. As shown in Table 1 and Figures S2, S3, S7, S9, and S11, changes in the size of the side chains do not lead to significant change in the spectroscopic properties of compounds with the same PAH core.

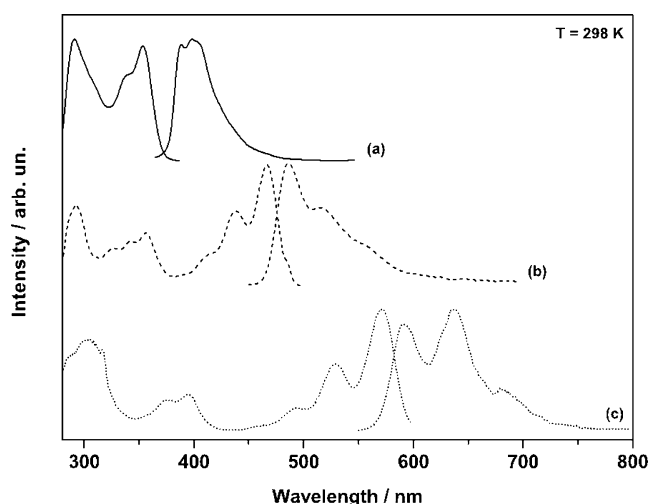


**Figure 3.** Excitation (left) and emission (right) spectra of a) **3a** (solid line;  $\lambda_{\text{exc}} = 353$  nm and  $\lambda_{\text{em}} = 389$  nm), b) **6b** (dashed line;  $\lambda_{\text{exc}} = 465$  nm and  $\lambda_{\text{em}} = 487$  nm), and c) **10a** (dotted line;  $\lambda_{\text{exc}} = 570$  nm and  $\lambda_{\text{em}} = 591$  nm) in toluene at 298 K.

In summary, we have developed a facile and efficient method for building pyrene, peropyrene, and teropyrene skeletons through a Brønsted acid promoted alkyne benzanulation strategy. Notably, no cyclodehydrogenation was involved to make the PAHs, and all the pyrenes, peropyrenes, and teropyrenes display good solubility in many common organic solvents. The UV/Vis absorption and fluorescence emission spectra show a gradual bathochromic shift as a function of increasing size of the  $\pi$  system. The successful synthesis of pyrenes, peropyrenes, and teropyrenes exemplifies the application of our method in the rapid construction of PAHs and suggest its potential use to synthesize larger fused ring systems with defined width, such as graphene nanoribbons. The ease of access of these new molecules will enable their synthesis and more importantly extensive characterization, as they are of potential interest for electronic and optoelectronic materials.

## Acknowledgements

W.A.C. acknowledges the Donors of the American Chemical Society Petroleum Research Fund for support of this research (PRF 53543-DN11). W.A.C. also thanks the University of Nevada, Reno for startup funds and the National Science Foundation for financial support through a CAREER Award (CHE-1555218). A.d.B.-D. acknowledges financial support through the NSF (CHE-1363325), and J.H.S.K.M. thanks CNPq (Conselho Nacional de Desenvolvimento Científico e Tecnológico—Brazil) for a Postdoctoral Fellowship (grant 232574/2014-6).

**Keywords:** alkynes · annulations · arenes · Brønsted acid · macrocycles

**How to cite:** *Angew. Chem. Int. Ed.* **2016**, *55*, 10427–10430  
*Angew. Chem.* **2016**, *128*, 10583–10586

- [1] a) J. Wu, W. Pisula, K. Müllen, *Chem. Rev.* **2007**, *107*, 718–747; b) S. Sergeyev, W. Pisula, Y. H. Geerts, *Chem. Soc. Rev.* **2007**, *36*, 1902–1929; c) S. Laschat, A. Baro, N. Steinke, F. Giesselmann, C. Hägele, G. Scalia, R. Judele, E. Kapatsina, S. Sauer, A. Schreivogel, M. Tosoni, *Angew. Chem. Int. Ed.* **2007**, *46*, 4832–4887; *Angew. Chem.* **2007**, *119*, 4916–4973; d) W. Pisula, X. Feng, K. Müllen, *Adv. Mater.* **2010**, *22*, 3634–3649; e) J. Mei, Y. Diao, A. L. Appleton, L. Fang, Z. Bao, *J. Am. Chem. Soc.* **2013**, *135*, 6724–6746; f) M. Ball, Y. Zhong, Y. Wu, C. Schenck, F. Ng, M. Steigerwald, S. Xiao, C. Nuckolls, *Acc. Chem. Res.* **2015**, *48*, 267–276; g) J. T. Markiewicz, F. Wudl, *ACS Appl. Mater. Interfaces* **2015**, *7*, 28063–28085; h) T. Wöhrle, I. Wurzbach, J. Kirres, A. Kostidou, N. Kapernaum, J. Litterscheidt, J. C. Haenle, P. Staffeld, A. Baro, F. Giesselmann, S. Laschat, *Chem. Rev.* **2016**, *116*, 1139–1241.
- [2] A. Narita, X.-Y. Wang, X. Feng, K. Müllen, *Chem. Soc. Rev.* **2015**, *44*, 6616–6643.
- [3] M. Grzybowski, K. Skonieczny, H. Butenschön, D. T. Gryko, *Angew. Chem. Int. Ed.* **2013**, *52*, 9900–9930; *Angew. Chem.* **2013**, *125*, 10084–10115.
- [4] T. J. Sisto, L. N. Zakharov, B. M. White, R. Jasti, *Chem. Sci.* **2016**, *7*, 3681–3688.
- [5] T. M. Figueira-Duarte, K. Müllen, *Chem. Rev.* **2011**, *111*, 7260–7314.
- [6] V. M. Nichols, M. T. Rodriguez, G. B. Piland, F. Tham, V. N. Nesterov, W. J. Youngblood, C. J. Bardeen, *J. Phys. Chem. C* **2013**, *117*, 16802–16810.
- [7] T. Umemoto, T. Kawashima, Y. Sakata, S. Misumi, *Tetrahedron Lett.* **1975**, *16*, 1005–1006.
- [8] a) B. L. Merner, L. N. Dawe, G. J. Bodwell, *Angew. Chem. Int. Ed.* **2009**, *48*, 5487–5491; *Angew. Chem.* **2009**, *121*, 5595–5599; b) B. L. Merner, K. S. Unikela, L. N. Dawe, D. W. Thompson, G. J. Bodwell, *Chem. Commun.* **2013**, *49*, 5930–5932.
- [9] N. Asao, T. Nogami, S. Lee, Y. Yamamoto, *J. Am. Chem. Soc.* **2003**, *125*, 10921–10925.
- [10] a) A. Fürstner, V. Mamane, *J. Org. Chem.* **2002**, *67*, 6264–6267; b) V. Mamane, P. Hannen, A. Fürstner, *Chem. Eur. J.* **2004**, *10*, 4556–4575; c) T. A. Chen, T. J. Lee, M. Y. Lin, S. M. Sohel, E. W. Diau, S. F. Lush, R. S. Liu, *Chem. Eur. J.* **2010**, *16*, 1826–1833.
- [11] a) A. Fürstner, V. Mamane, *Chem. Commun.* **2003**, 2112–2113; b) R. Stężycki, M. Grzybowski, G. Clermont, M. Blanchard-Desce, D. T. Gryko, *Chem. Eur. J.* **2016**, *22*, 5198–5203.
- [12] S. Yamaguchi, T. M. Swager, *J. Am. Chem. Soc.* **2001**, *123*, 12087–12088.
- [13] a) M. B. Goldfinger, T. M. Swager, *J. Am. Chem. Soc.* **1994**, *116*, 7895–7896; b) M. B. Goldfinger, K. B. Crawford, T. M. Swager, *J. Am. Chem. Soc.* **1997**, *119*, 4578–4593; c) T. Yao, M. A. Campo, R. C. Larock, *J. Org. Chem.* **2005**, *70*, 3511–3517; d) A. Mukherjee, K. Pati, R.-S. Liu, *J. Org. Chem.* **2009**, *74*, 6311–6314.
- [14] a) D. B. Walker, J. Howego, A. P. Davis, *Synthesis* **2010**, 3686–3692; b) T. Matsuda, T. Moriya, T. Goya, M. Murakami, *Chem. Lett.* **2011**, *40*, 40–41.
- [15] For another example of this deshielding effect, see: M. Kastler, J. Schmidt, W. Pisula, D. Sebastiani, K. Müllen, *J. Am. Chem. Soc.* **2006**, *128*, 9526–9534.
- [16] a) S. C. Martens, T. Riehm, S. Geib, H. Wadepohl, L. H. Gade, *J. Org. Chem.* **2011**, *76*, 609–617; b) S. Chen, F. S. Raad, M. Ahmida, B. R. Kaafarani, S. H. Eichhorn, *Org. Lett.* **2013**, *15*, 558–561.

Received: May 15, 2016  
Published online: July 26, 2016